Thermochimica Acta 603 (2015) 123–127

Contents lists available at ScienceDirect

Thermochimica Acta

journal homepage: www.elsevier.com/locate/tca

Measurement of the limiting fictive temperature over five decades of cooling and heating rates

Siyang Gao, Sindee L. Simon *

Department of Chemical Engineering, Texas Tech University, Lubbock, TX 79409-3121, USA

ARTICLE INFO

Article history:
Available online 20 August 2014

Keywords:
Glass transition temperature
Limiting fictive temperature
Cooling and heating rate dependence
WLF equation
Polystyrene

ABSTRACT

The fictive temperature (T_f) was defined by Tool in the 1940s as a measure of glassy structure. T_f is generally measured on heating and can be calculated from the enthalpy overshoot in calorimetric studies using a method developed by Moynihan. Prior work has demonstrated that the limiting fictive temperature (T_f') is similar to T_g (measured on cooling) and depends on the cooling rate in a manner consistent with the Williams–Landel–Ferry (WLF) relationship. Theoretically, the limiting fictive temperature should not depend on heating rate, but this has been experimentally verified only for a very limited range of heating rates. Here, rapid-scanning chip calorimetry and conventional differential scanning calorimetry (DSC) are combined to investigate T_f' for polystyrene over a broad range of heating rates ranging from 0.017 to 3000 K/s after cooling at different rates. The results show that T_f' depends on cooling rate following the WLF equation. On the other hand, T_f' is not a function of heating rate, consistent with theoretical predictions, in spite of the change in the magnitude and placement of the enthalpy overshoot.

1. Introduction

The glass transition temperature, T_g, is an important property of glass-forming materials and often defines temperature ranges for application and processing. By definition, T_g is a measure of the temperature range where vitrification occurs on cooling from the liquid state, and it is often taken as the midpoint of this range and defined as the intersection of the extrapolated glass and liquid lines made on cooling [1–3]. Since the transition is a kinetic rather than dynamic process, T_g depends on the rate of cooling following the well-known Williams–Landel–Ferry (WLF) [4] and Vogel–Fulcher–Tammann (VFT) [5–7] behavior.

On the other hand, the fictive temperature, T_f, is generally measured on heating and was introduced by Tool [8] as a measure of glass structure or the distance of a glass from its equilibrium state. In enthalpy space, T_f is defined as the intersection of the glass and liquid lines obtained on heating, which depends on cooling rate (q), as shown in Fig. 1. The glass lines move to lower enthalpies (and lower volumes) as the cooling rate decreases due to the increased time for relaxation; on heating, as shown, the enthalpy for the lowest cooling rates overshoots the liquid line resulting in a maximum or peak in the heat capacity. The overshoot observed on heating is well understood [3], and the overshoot increases as the ratio of the heating rate to the preceding cooling rate increases.

In the case of an unaged glass, T_f is termed the limiting fictive temperature T_f'. The importance of T_f' is its equivalence to T_g [9–12]. Due to instrumental limitations, early researchers performed calorimetric measurements only on heating, and thus, often referred to T_f' as T_g [13,14]. The measurement of T_g has become further confused by industrial practices [1], such as ASTM E 1356-08 [15], which defines various glass transition temperatures, including an extrapolated end temperature and inflection temperature. As indicated in the schematic Fig. 1, there can be significant differences between T_f' and the position of the enthalpy overshoot. Furthermore, because of the kinetics associated with the glass transition, the devitrification transition measured on heating depends on the heating rate, leading researchers to incorrectly assert that T_g depends on the heating rate. In fact, neither T_g nor T_f' should theoretically depend on heating rate. Rather, both should only depend on the cooling rate – and this dependence on cooling rate has been verified [9–12]. However, the lack of a dependence of T_f' on heating rate has been investigated only for a limited range of heating rates from 5 to 40 K/min [11]. Here, we extend such measurements to a much broader range of heating and cooling rates to verify the dependence of T_f' on these variables. In particular, we study a high molecular weight polystyrene with both conventional and Flash DSC using heating rates ranging from 0.017 to 3000 K/s, over five decades, after cooling at rates ranging

* Corresponding author. +1 806 834 8470/742 1763.
E-mail address: sindee.simon@ttu.edu (S.L. Simon).

http://dx.doi.org/10.1016/j.tca.2014.08.019
0040-6031/

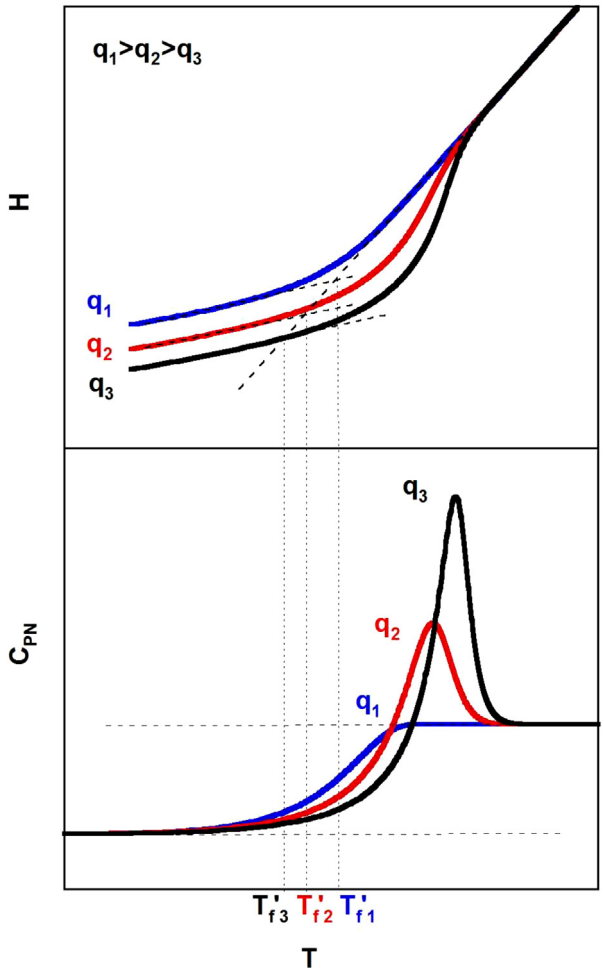

Fig. 1. Schematic plot of the enthalpy (H) and normalized heating capacity (C_{PN}) versus temperature when heating at the same rate after cooling at different rates, q_1, q_2, q_3, respectively, where $q_1 > q_2 > q_3$. The limiting fictive temperature is determined from the intersection of the glass and liquid lines resulting in $T_f'_1 > T_f'_2 > T_f'_3$ in spite of the overshoot shift to higher temperatures for lower q values. Volume and thermal expansivity plots are analogues.

over nearly six decades from 0.0017 to 1000 K/s. The dependence of the limiting fictive temperature on cooling rate and its independence on heating rate are confirmed and discussed.

2. Methodology

Polystyrene (Sigma–Aldrich) with 1,998,000 g/mol number-average molecular weight and PDI of 1.02 is used in this study. This material has been used previously in our laboratory and its T_g behavior has been characterized [16–18].

A Mettler Toledo Flash DSC was used with a freon intercooler with nitrogen purge. The sensor support temperature (T_{ss}) was set at −100 °C. The Flash DSC sample was a 160 nm-thick polystyrene film, spin-cast from toluene (99.999% purity, Sigma–Aldrich) using a 0.91 wt% concentration. The thickness was determined by atomic force microscope (AFM, Advanced Scanning Probe Microscope XE-100) in tapping mode after making a scratch on the film supported by a glass substrate. After spincoating, the film was floated on water to separate it from the mica substrate, and then picked up with mesh wire. The sample was annealed under ambient environment for 24 h, followed by another 24 h under vacuum at 50 °C. The film was then cut to a ~0.2 mm × 0.2 mm piece under a microscope and picked up by a hair pen to transfer it on the center of the sensor chip, which contained a thin layer of Krytox oil (DuPontTM, T_g = −63.2 °C) to enhance the thermal conductivity. The Krytox oil is inert to the polystyrene sample over several months based on measurements in our laboratory [19–21]. Heating rates (β) of 3000, 1000, and 300 K/s were employed from 35 to 180 °C after cooling at five different rates from 0.1 to 1000 K/s. Three runs were performed at each heating rate to check reproducibility.

For conventional DSC, a Mettler Toledo DSC 1 with intracooler at 5 °C and a DSC 823 with freon cooler at −80 °C were employed for this study, both with nitrogen gas purge. For these studies, the polystyrene was molded to a 1 mm thick sample to ensure good thermal contact with the standard aluminum DSC pan. The sample was heated from 25 to 150 °C at four different heating rates from 0.017 to 0.5 K/s (1–30 K/min) after cooling at rates ranging from 0.0017 to 0.5 K/s (0.1–30 K/min) for the DSC 1 and after cooling at a rate of 1 K/s (60 K/min) for the DSC 823. Three runs were also conducted at each heating rate to check reproducibility.

The limiting fictive temperatures were calculated from the heating scans using Moynihan's method [14] for both Flash DSC and conventional data:

$$\int_{T_{f'}}^{T \gg T_g} (C_{pl} - C_{pg})dT = \int_{T \ll T_g}^{T \gg T_g} (C_p - C_{pg})dT \quad (1)$$

where C_{pl} and C_{pg} are the liquid and glass heat capacities, C_p is the heat capacity of the sample. The methodology is illustrated in Fig. 2 for heating rates of 3000 and 0.17 K/s from Flash and conventional DSC, respectively, both obtained after cooling at 0.1 K/s. The limiting fictive temperature T_f' is determined by equating areas A_1 and A_2 as shown in Fig. 2. The glass and liquid lines for scans with a given heating rate are well superposed far from the transition in both glass and liquid region by minimizing χ^2 (shown later). This methodology reduces the error in the limiting fictive temperature calculation because it results in a consistent liquid line for the integration, and it is especially important for curves having large enthalpy overshoots, for example, on heating after a very low cooling rate [18]. When the enthalpy overshoot is large and the T_f' value is lower than the onset of devitrification, as shown for the first heat capacity curve obtained at 3000 K/s heating rate, a

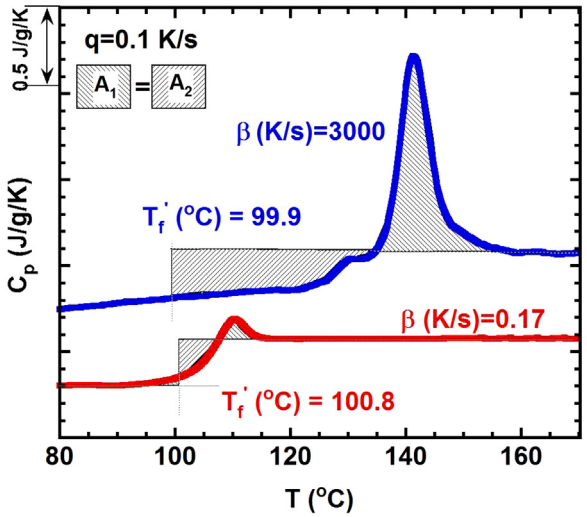

Fig. 2. Heat flow in heat capacity units for polystyrene from Flash and conventional DSC heating curves obtained at heating rates of 3000 and 0.17 K/s, respectively, after cooling at 0.1 K/s. The step change in heat capacity at 100 °C for the Flash DSC sample is assumed to be the same as that measured using conventional DSC. Curves were rotated to be horizontal in the liquid state.

simplified method involving only the liquid line is required [18]. However, for the case when the T_f' value is higher than the onset of the glass transition, as in the conventional DSC curve for $\beta = 0.17$ K/s, both glass and liquid lines are required to calculate the T_f' value. The standard deviations of the T_f' values from Flash DSC and conventional DSC measurements ranged from 0.4 to 0.8 K and from 0.2 to 0.6 K, respectively, with the highest standard deviations typically observed at the lowest heating rates.

In the case of substantive thermal gradients in the DSC sample, T_f' values must be corrected: we find that T_f' is shifted by the average thermal gradient in the sample at the onset of devitrification (i.e., in the glass state), based on analysis of DSC enthalpy overshoots calculated with and without taking into account thermal gradients [22]. For the Flash DSC sample, the thermal lag in a 160 nm thick film is negligible (less than 1×10^{-5} K) even at our highest heating rate of 3000 K/s according to calculations based on a model of the thermal gradients [22], and also consistent with recent published work by Schawe in this issue [23]. In that latter study, a 10 μm thick polystyrene film showed an average temperature 1.25 K lower than the program temperature on heating at 3000 K/s [23]; our 160 nm thick film would be expected to have an average thermal gradient 10^{-4} times lower than this. Hence, no corrections for thermal gradient effects are needed for T_f' values obtained from Flash DSC experiments due to the thin sample size.

Concerning the thermal gradients in our conventional DSC sample, the average sample temperature is calculated to be approximately 0.4 and 0.8 K lower than the program temperature in the glassy state near T_g for heating rates of 0.17 and 0.5 K/s (10 and 30 K/min), again based on a model [22] of the thermal gradient. This contrasts with much larger gradients reported by Schawe [23] based on a comparison of T_g measured on cooling and T_f' measured on heating. However, we performed similar experiments as those performed by Schawe, and, for our sample, the results show that T_g (from the midpoint in C_p) is 0.96 K higher than T_f' for 10 K/min cooling and heating rates, rather than $T_g < T_f'$ due to thermal gradients. Schawe [23] used T_g as defined by the Richardson method [24], which is analogous to Eq. (1); in that case, our T_g is 0.88 K higher than T_f'. The finding here of $T_g > T_f'$ was observed in prior work from our laboratory using both calorimetry and dilatometry and was attributed to a broad transition on cooling [12]. The result has also been reproduced by modeling [12,25]. The apparent discrepancy with Schawe's results may arise from differences in sample thermal contact but it does not seem to be related to the definition of T_g. Since we cannot estimate the thermal gradient using Schawe's method, we correct the results based on the calculated gradients: the T_f' values reported in this study were corrected by 0.4 and 0.8 K for heating rates of 0.17 and 0.5 K/s. For heating rates of 0.05 K/s (3 K/min) and lower, the average temperature in the sample is calculated to be less than 0.12 K lower than the program temperature at T_g, and hence, no corrections were made.

The temperature calibration was performed for Flash DSC by matching our T_f' data obtained on heating at 600 K/s with previous data obtained at the same rate for four different polystyrene films for which the temperature of each was calibrated with indium [25]. A correction to the temperature calibration was made for other heating rates by examining the heating rate dependence of the melting point for a piece of indium place on top of a 160 nm thick polystyrene film. The onset melting temperature of the indium linearly increases by 2.5 K as heating rate increases from 1 to 3000 K/s, and the temperature is corrected accordingly. For conventional DSC, the temperature calibration was performed on heating with indium at 0.17 K/s. The onset melting temperature of the indium linearly increases by 1.9 K as heating rate increases from 0.0017 to 0.5 K/s, and the temperature is corrected accordingly. To perform experiments on cooling to determine if we could estimate the thermal gradient as in Ref. [23], the temperature was also calibrated on cooling at 10 K/min using two liquid crystal standards, CE-3 (Chromophone, Inc.) and 4,4-azoxyanisole (Sigma–Aldrich).

3. Results

Typical flash DSC heat flow scans for the 160 nm polystyrene film are shown in Fig. 3 as a function of cooling rate, with the upper panel showing results for a heating rate β of 3000 K/s, and lower panels showing those for 1000 and 300 K/s, respectively. The enthalpy overshoot shifts to higher temperatures and grows in magnitude with decreasing cooling rate for all heating rates, as expected [12].

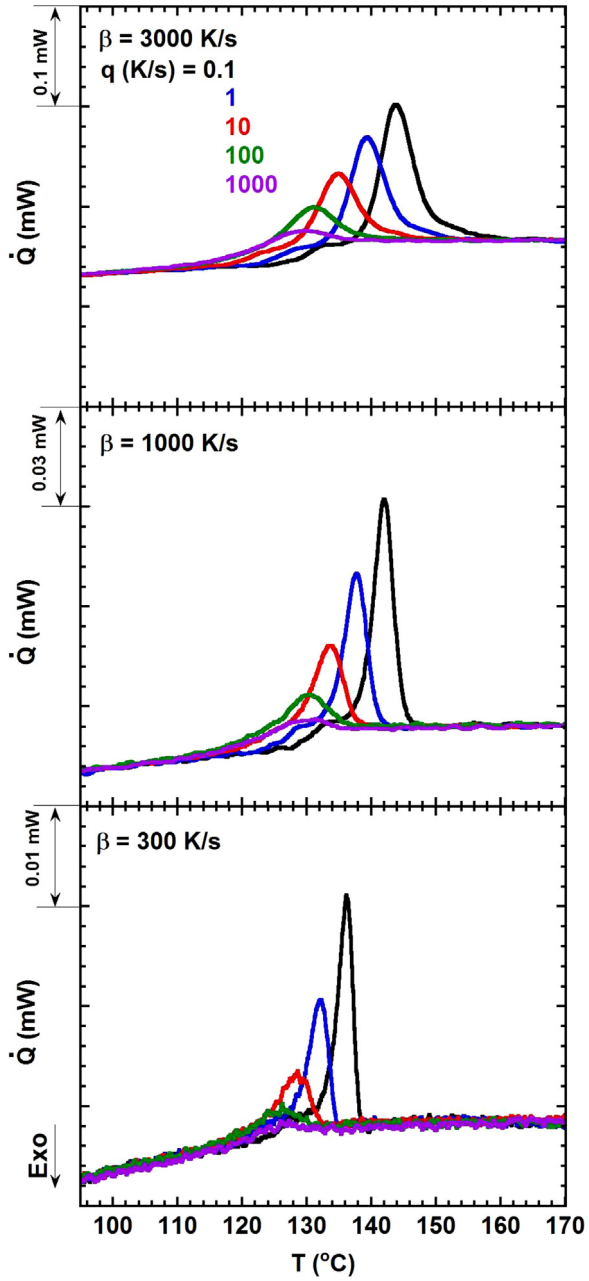

Fig. 3. Flash DSC heating scans for polystyrene as a function of cooling rate (q) for heating rates at 3000, 1000, and 300 K/s, from top to bottom. Curves were superposed and rotated to be horizontal in the liquid state. View in color for best clarity.

Comparing the panels, the overshoots shift to lower temperatures, and the breadths and areas decrease as the heating rate decreases because the sample has more time recover to the liquid line in a given temperature range for lower heating rates. It should be clear to the reader based on these results that the point of devitrification on heating depends on both the cooling and heating rate, although the point of vitrification (i.e., the glass transition, T_g) is only a function of the cooling rate from the liquid state. In addition, the reader should notice that experimental data for both liquid and glass lines superpose very well for all scans made at a given rate; this is important for drawing an unbiased and consistent liquid line and reduces the error inT_f'.

Typical conventional DSC heat flow scans for the polystyrene sample are similarly shown in Fig. 4 as a function of cooling rate. The uppermost panel is for a heating rate β of 0.5 K/s. The lower panels show results for heating rates of 0.17, 0.05, and 0.017 K/s. The enthalpy overshoots show the same trends as for the Flash DSC heating curves, shifting to higher temperatures and growing in magnitude with decreasing cooling rate. The placement of the enthalpy overshoot also shifts to lower temperatures, and its breadth and area decrease as heating rate decreases. Again, both liquid and glass lines superpose very well for all scans made at a given heating rate.

The T_f' values are plotted as a function of heating rate in Fig. 5 for four representative cooling rates. Within the error of the measurements (with standard deviations ranging from 0.2 to 0.8 K), the values of T_f' for a given cooling rate are the same, independent of heating rate. This is despite the associated changes in the shape and the placement of the enthalpy overshoot, as were show in Fig. 2. On the other hand, the limiting fictive temperature T_f' is clearly a function of cooling rate, increasing with increasing cooling rate. Fig. 6 shows the data plotted versus the logarithm of the cooling rate for all heating rates studied. The Williams–Landel–Ferry (WLF) equation [4] is used to describe the cooling rate dependence of T_f':

$$\log\left(\frac{q}{q_{\mathrm{ref}}}\right) = \frac{C_1(T_{f'} - T_{f'\,\mathrm{ref}})}{C_2 + (T_{f'} - T_{f'\,\mathrm{ref}})} \tag{2}$$

where q is the cooling rate, q_{ref} is the reference cooling rate of 0.1 K/s, $T_{f'\,\mathrm{ref}}$ is the limiting fictive temperature at the reference cooling rate (373.3 K), and C_1 and C_2 are constants. The fit well describes the data with $C_1 = 12.8$ and $C_2 = 47.9$ K. We used a "nominal" $T_{f'\,\mathrm{ref}}$ value in Eq. (2) in order to easily compare the results with those in the literature since C_1 and C_2 depend on the choice of the reference temperature. The fragility m can be also calculated from this equation [26]:

$$m = -\frac{\mathrm{d}\log q}{\mathrm{d}\left(\frac{T_{f'\,\mathrm{ref}}}{T_{f'}}\right)} = \frac{T_{f'\,\mathrm{ref}}C_1}{C_2} \tag{3}$$

The fragility obtained of 99.8 ± 2.1 is similar to that of the bulk and thick ultrathin film samples that we previously reported [18].

4. Discussion

A small and consistent bump or sub-peak prior to the glass transition peak was observed using Flash DSC for each heating curve after cooling at the lowest cooling rates, but the bump is not observed after cooling at high rates, as shown in Fig. 3. Such phenomenon is not observed for conventional DSC data. However, a similar response was observed in our previous Flash DSC study for samples directly spincast on the back of the sensor after slow cooling [18]. In that work [18], we discussed the possibility of residual or thermal stresses causing such sub-peaks, but we ruled out this cause for our samples. The origin of the sub-peaks still remains unclear.

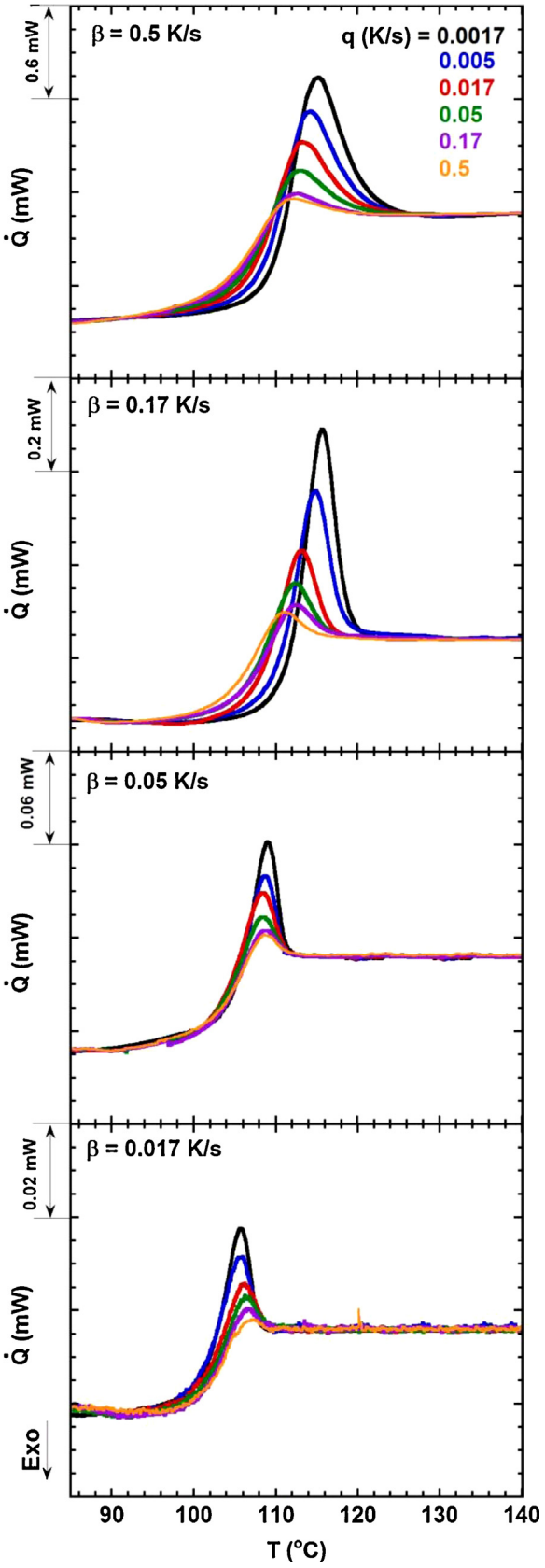

Fig. 4. Conventional DSC heating scans for polystyrene as a function of cooling rate (q) for heating rates of 0.5, 0.17, 0.05, and 0.017 K/s, from top to bottom. Curves were superposed and rotated to be horizontal in the liquid state. View in color for best clarity.

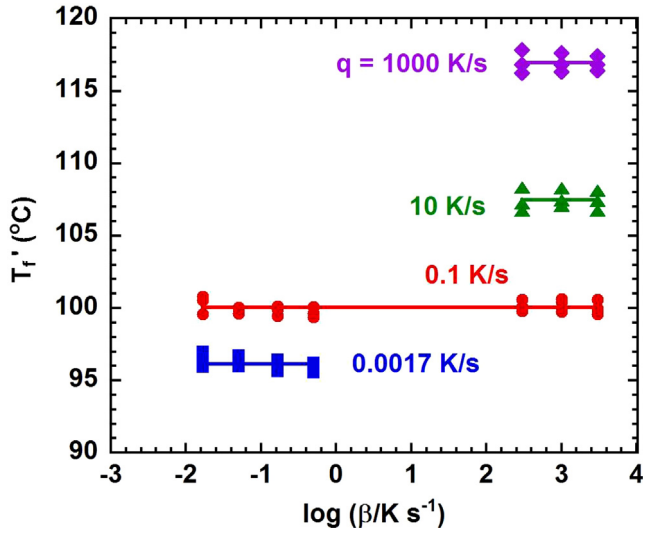

Fig. 5. The limiting fictive temperature versus logarithm of the heating rate (β) after cooling at rate q of 0.0017, 0.1, 10, and 1000 K/s. The solid line is the average T_f' for each q value.

The heat capacity curves shown in Fig. 2 illustrate that the enthalpy overshoot shifts to higher temperatures and grows in magnitude as heating rate increases for a given cooling rate. The interesting point is that although the shape and placement of the overshoots differ, with a 20 K change in the onset of devitrification, the two curves give the same T_f' value within 1 K. The results shown in Figs. 5 and 6, also conclusively demonstrate that the limiting fictive temperature does not depend on heating rate. This is consistent with the theoretical expectation and with previous results [11] for a heating rate range of less than one decade. The results further demonstrate the importance of correctly calculating T_f' from DSC heating curves that display enthalpy overshoots. Errors of over 20 K can be incurred by equating T_g to the onset of devitrification when large overshoots exist.

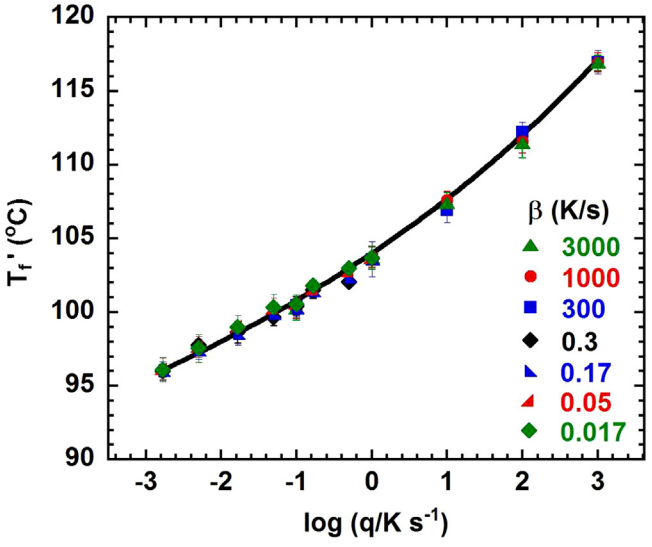

Fig. 6. The limiting fictive temperature versus logarithm of the cooling rate (q) as a function of different heating rates from 0.017 to 3000 K/s. The solid line represents the best fit to the WLF equation.

5. Conclusion

The limiting fictive temperature T_f' of a high molecular weight polystyrene was measured on heating for a range of heating rates covering over five decades. Enthalpy overshoots were found shift to higher temperatures and grow in magnitude with decreasing cooling rate for all heating rates. In addition, the overshoots shift to lower temperatures, and the breadths and areas decrease as the heating rate decreases. The values of T_f' for a given cooling rate are the same within the error of the measurements (with standard deviations ranging from 0.2 to 0.8 K), independent of heating rate. The limiting fictive temperature T_f' depends on cooling rate, following the Williams–Landel–Ferry (WLF) relationship.

Acknowledgements

The authors gratefully acknowledge funding from NSF and DMR1006972.

Reference

[1] J.M. Hutchinson, Physical aging of polymers, Prog. Polym. Sci. 20 (1995) 703–760.
[2] D.J. Plazek, K.L. Ngai, The glass temperature, in: J.E. Mark (Ed.), Physical Properties of Polymers Handbook, AIP Press, New York, 1996, pp. 139–159.
[3] G.B. McKenna, S.L. Simon, The glass transition: its measurement and underlying physics, in: S.Z.D. Cheng (Ed.), Handbook of Thermal Analysis and Calorimetry, Elsevier, New York, 2002, pp. 49–109.
[4] M.L. Williams, R.F. Landel, J.D. Ferry, The temperature dependence of relaxation mechanisms in amorphous polymers and other glass-forming liquids, J. Am. Chem. Soc. 77 (1955) 3701–3707.
[5] H. Vogel, The law of viscosity-temperature dependence of fluids, Phys. Z. 22 (1921) 645–646.
[6] G.S. Fulcher, Analysis of recent measurements of the viscosity of glasses, J. Am. Ceram. Soc. 8 (1925) 339–355.
[7] G.Tammann,Glassesassupercooledliquids,J.Soc.GlassTechnol.9(1925)166–185.
[8] A.Q. Tool, Relation between inelastic deformability and thermal expansion of glass in its annealing range, J. Am. Ceram. Soc. 29 (1946) 240–253.
[9] D.J. Plazek, Z.N. Frund Jr., Epoxy resins (DGEBA): the curing and physical aging process, J. Polym. Sci. B: Polym. Phys. 28 (1990) 431–448.
[10] D.J. Plazek, I.C. Choy, The physical properties of bisphenol-A-based epoxy resins during and after curing. II. Creep behavior above and below the glass transition temperature, J. Polym. Sci. Part B: Polym. Phys. 27 (1989) 307–324.
[11] M.J. Richardson, N.J. Savill, Derivation of accurate glass transition temperatures by differential scanning calorimetry, Polymer 16 (1975) 753–757.
[12] P. Badrinarayanan, W. Zheng, Q.X. Li, S.L. Simon, The glass transition temperature versus the fictive temperature, J. Non-Cryst. Solids 353 (2007) 2603–2612.
[13] C.T. Moynihan, A.J. Easteal, J. Wilder, Dependence of the glass transition temperature on heating and cooling rate, J. Phys. Chem. 78 (1974) 2673–2677.
[14] C.T. Moynihan, A.J. Easteal, M.A. DeBolt, J. Tucker, Dependence of the fictive temperature of glass on cooling rate, J. Am. Ceram. Soc. 59 (1976) 12–16.
[15] ASTM E1356, Standard Test Method for Assignment of the Glass Transition Temperatures by Differential Scanning Calorimetry, 08 (2014) 1–4.
[16] Y.P. Koh, G.B. McKenna, S.L. Simon, Calorimetric galss transition temperature and absolute heat capacity of polystyrene ultrathin film, J. Polym. Sci. Part B: Polym. Phys. 44 (2006) 3518–3527.
[17] Y.P. Koh, S.L. Simon, Structural relaxation of stacked ultrathin polystyrene films, J. Polym. Sci. Part B: Polym. Phys. 46 (2008) 2741–2753.
[18] S.Y. Gao, Y.P. Koh, S.L. Simon, Calorimetric glass transition of single polystyrene ultrathin films, Macromolecules 46 (2013) 562–570.
[19] J.X. Guo, S.L. Simon, Effect of crosslink density on the pressure relaxation response of polycyanurate networks, J. Polym. Sci. Part B: Polym. Phys. 47 (2009) 2477–2486.
[20] J.X. Guo, S.L. Simon, Pressure–volume–temperature behavior of two polycyanurate networks, J. Polym. Sci. Part B: Polym. Phys. 48 (2010) 2509–2517.
[21] J.X. Guo, L. Grassia, S.L. Simon, Pressure–volume–temperature behavior of two polycyanurate networks, J. Polym. Sci. Part B: Polym. Phys. 50 (2012) 1233–1244.
[22] S.L. Simon, Enthalpy recovery of poly(ether imide): experiment and model calculations incorporating thermal gradients, Macromolecules 30 (1997) 4056–4063.
[23] J.E.K. Schawe, Measurement of the thermal glass transition of polystyrene in a cooling rate range of more than 6 decades, Thermochimica. Acta 603 (2015) 128–134.
[24] M.J. Richardson, N.G. Savill, Derivation of accurate glass transition temperatures by differential scanning calorimetry, Polymer 16 (1976) 753–757.
[25] Y.P. Koh, L. Grassia, S.L. Simon, Structural recovery of a single polystyrene thin film using nanocalorimetry to extend the aging time and aging temperature range, Thermochimica. Acta 603 (2015) 135–141.
[26] C.A.A. Angell, Relaxation in liquids, polymers and plastic crystals – strong/fragile patterns and problems, J. Non-Cryst. Solids 131 (1991) 13–31.